研 究 速 報

Finite Element Analysis of Velocity Distribution in Bearing Section during Extrusion of Rectangular, Angle and Channel Sections

—Combination of Numerical Analysis and Die Design-2—

矩形材，アングル材，チャンネル材押出し加工時のダイスベアリング部での塑性流動

—数値解析技術とダイス設計との結合法- 2 —

Manabu KIUCHI*, Jun YANAGIMOTO* and Victor MENDOŻA*

木　内　　学・柳　本　　潤・ヴィクトール　メンドーサ

1. Introduction

The present work is continuation of[1),2)]. In[1)] the method developed for the analysis of the problem of balancing the material flow was presented and its applicability was shown by carrying out simulations of extrusion process of rectangular sections. In[2)] the applicability was extended to more complex sections such as angle and channels and it was shown that the exit velocities were very sensitive to the position of the die opening and the length of the bearing land. This time, the number of simulated cases is increased and the influence of the position of the die opening, length of the bearing land as well as the extrusion ratio is studied.

2. Extrusion Process Simulation

The geometry of the simulated profiles are the same as those of[1),2)] as well as the process conditions used in the simulations. The exceptions are the length of the bearing land and the extrusion ratio. In this work, the length of the bearing land used in the simulations are: $Z_B = 5, 7.5, 10$ and 12.5 mm. With respect to the extrusion ratio, the simulated values are: $ER = 39, 90, 139, 185, 260, 325$ and 360.

3. Results and Discussions

Fig. 1 shows the variation of P_{Av} (Average Extrusion Pressure) and *SDV* (Standard Deviation of the axial Velocity, V_Z) with *EC* (Eccentricity of the die opening) and *AR* (aspect ratio of the section). The values of *SDV* are those corresponding to the cross sectional plane at the die entrance. As could be expected P_{Av} increases with *AR*, however, *SDV* is markedly higher for lower AR sections. This behavior can be explained by considering that for a section with *AR* near 1, the difference in distance traveled by different material points before they reach the die entrance is bigger compared with higher *AR* sections.

Fig. 2 shows the variation of *SDV* along the axial position of the bearing for 5.0 mm bearing length cases. It is observed that, although the sections with higher *AR* have lower *SDV* from the die entrance, the distribution of the axial velocity needs longer distance to become uniform. Also, it is seen that, when $EC = 0$, all the sections come out with uniform axial velocity. This figure shows also the sensitivity of *SDV* with *AR*. That is, the higher the *AR* the higher the sensitivity of *SDV* to EC changes.

With respect to the effect of Z_B on P_{Av}, **Fig. 3** shows the results for a section with $AR = 2$ and various *EC* values. As expected, P_{Av} increases with Z_B, however, the effect is not so pronounced compared with the effect of *EC* and *AR*. In fact, the results showed until now, indicate that the most influential parameter on both P_{Av} and *SDV* is *EC*.

In this work *SDV* is used as a measure of uniformity of V_Z, however, it does not show the shape of the velocity distribution. In **Fig. 4** are shown 3-D plots of V_Z for a section with $AR = 8$, the value for *EC* is -20 mm and Z_B is 5 mm. Two plots are shown **(a)** at the die-entrance and **(b)** at the die-exit. The plots indicate the fact that the metal flow is suppressed by the die wall in the inlet region, however, in the outlet region the metal slides well against the die wall. Between these two regions there is a kind of partial-sticking

*2nd Department, Institute of Industrial Science, University of Tokyo

/ sliding transition region. In the sticking region there is a layer of metal adjacent to the surface, which moves with a considerable lower velocity. Towards the die exit, the sliding region, V_Z tends to become uniform, however, in the present situation, the bearing length is too short to reach uniform V_Z across the cross-section, therefore, the material exits in bending fashion.

In **Fig. 5** the ordinate corresponds to *SDV* at certain position divided by the average axial velocity of the product and the abscissa to the position along bearing length. The effect of *ER* on *SDV* behavior can be clearly seen. The plot shows the interesting fact that as *ER* increases the necessary bearing length to get uniform axial velocity at the die exit decreases.

The influence of *EC* and Z_B on P_{Av} and *SDV* in extrusion of angle sections is shown in **Fig. 6**. The effect can be clearly appreciated. Due to the geometric characteristics of these sections, the plots show minimum P_{Av} and *SDV* indicating

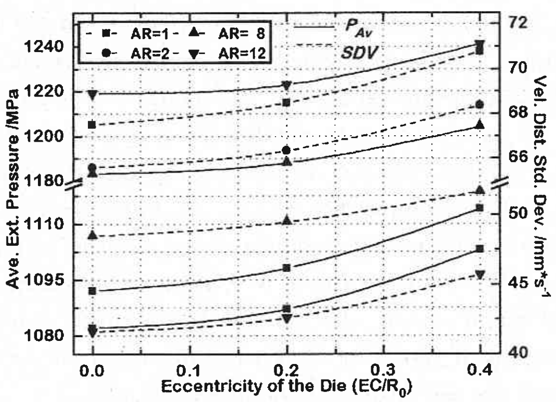

Fig. 1 Variation of P_{Av} and *SDV* at die entrance with *EC* and *AR* for rectangular sections, Z_B = 5 mm

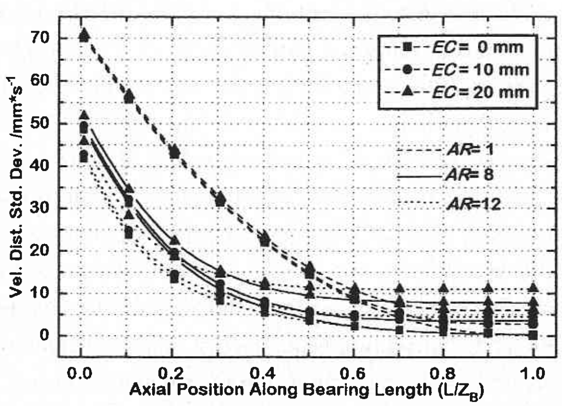

Fig. 2 Effect of *AR* and *EC* on *SDV* along bearing length for rectangular sections, Z_B = 5 mm.

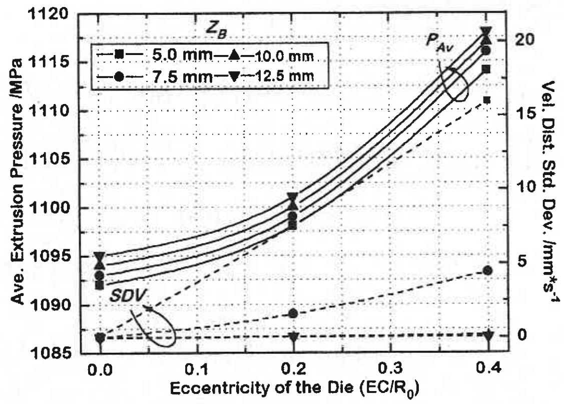

Fig. 3 Effect of Z_B and *EC* on P_{Av} and *SDV* at die exit for a rectangular section, *AR* =4 2

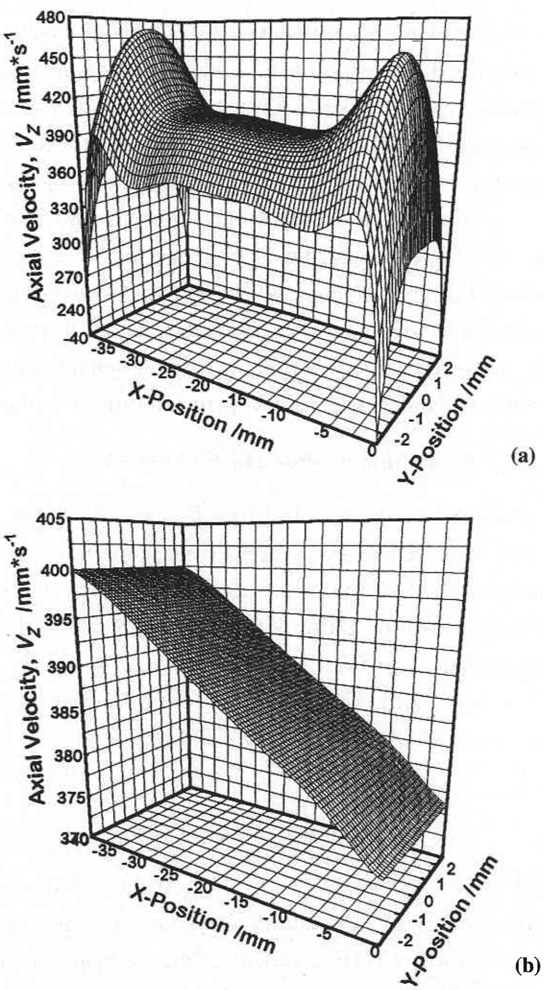

Fig. 4 Axial velocity distribution for a rectangular section, *AR* = 8, *EC* = −20 mm, Z_B = 5 mm **(a)** die entrance **(b)** die exit.

that there is an optimal EC where the P_{Av} required for the process is minimum as well as the nonuniformity of the velocity distribution is minimum, i.e., SDV has the lowest value. For the angle section with $AR = 12$, the optimal eccentricity in terms of P_{Av} coincides with the gravity center position, indicated by the dropped line. In reference to SDV the minimum of the curves are slightly displaced towards more negative values. The same behavior was observed for sections with $AR = 8$, both angles and channels.

For lower AR sections, the behavior showed is different. **Fig. 7** shows the results for an angle section with $AR = 2$. Again, the optimum EC in terms of P_{Av} coincides with the position of the gravity center, however, with respect to SDV the minimum values are markedly displaced towards positive values.

In extrusion die design well detailed knowledge of V_Z distribution is desirable, e.g., where the fastest velocities are taking place and how it changes with other extrusion parameters. **In Fig. 8** are shown the V_Z profiles for an angle section with $AR = 8$ and $EC = -10$ mm. The positions correspond to the planes located at the entrance and at the exit of the die for a $Z_B = 10$ mm case. In this case, the bearing land is long enough and the metal shows almost constant V_Z across the cross section that corresponds to the straightness.

Other important characteristics of the metal flow due to the differences in die design can be better appreciated, for example, by tracing the stream-lines patterns. **Fig. 9** shows the results for an angle section with $AR = 8$ and $EC = -10$ mm. Z_B is 5 and 10 mm in the stream-lines patterns shown in **(a)** and **(b)**, respectively. The plots show that when Z_B is 5 mm the metal comes out not straightly, but in $Z_B = 10$ mm case the product exits with acceptable straightness. Moreover, by observing the stream-lines patterns, it is possible to appreciate the shape and the relative size of the dead metal zone as well as the curvature of the product.

The relationship between P_{Av} and ER is illustrated in **Fig. 10**. P_{Av} increases with ER, but not a great variation is shown with respect to the geometry of the section.

Extrusion die-design aims to get a product without both geometrical and structural defects. The mean stress, σ_m, has been shown to play an important role in the occurrence of central-bursting cracks. A study of this component may be interest in extrusion to determine the factors leading with central defects. σ_m distributions at the Z-X plane corresponding to the central position are shown in **Fig. 11** for a rectangular section. The distribution shows in $ER = 39$ case that mean stresses are all compressive in central zone.

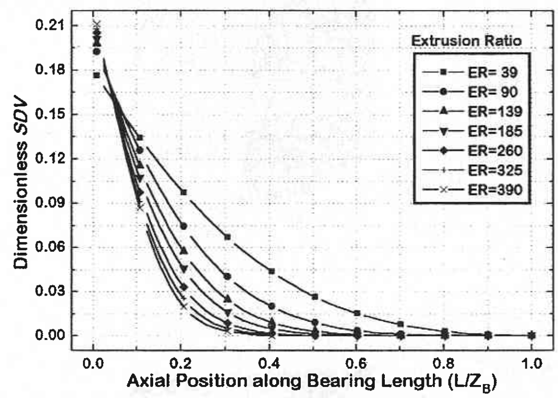

Fig. 5 Effect of ER on SDV for a rectangular section, $AR = 1$, $Z_B = 5$ mm.

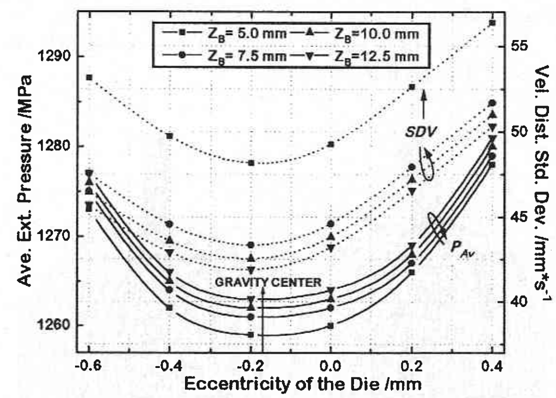

Fig. 6 Variation of P_{Av} and SDV at the die entrance with EC and Z_B for an angle section, $\alpha = 120$, $AR = 12$.

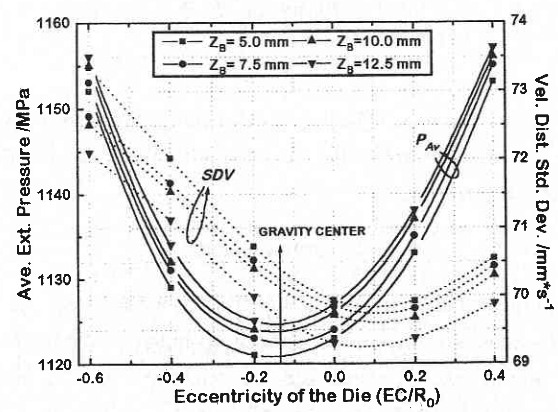

Fig. 7 Variation of P_{Av} and SDV at the die entrance with EC and Z_B for an angle section, $\alpha = 120$, $AR = 2$.

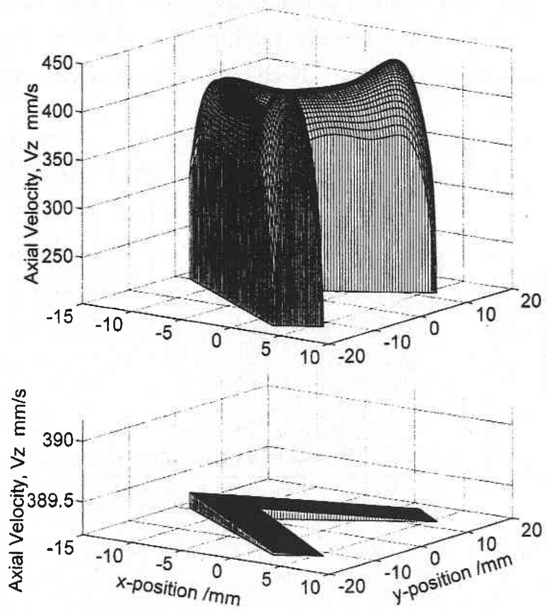

Fig. 8 Axial velocity profiles for an angle section, α = 900, AR = 8, EC = −10 mm, Z_B = −10 mm **(a)** die entrance **(b)** die exit.

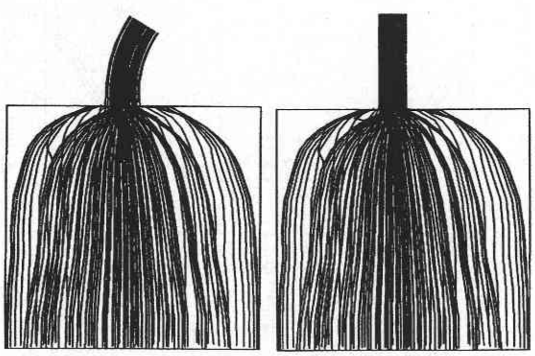

Fig. 9 Stream lines for an angle section, α = 90 , AR = 8, EC = −10 mm **(a)** Z_B = 5 mm **(b)** Z_B = 10 mm.

However, in ER = 390 case, tensile values are developed in the central zone indicating the possibility of center-bursting cracks occurrence.

4. Conclusions

Numerical analysis shows that there is a zone near the die entrance where the contact conditions between die land and the metal are characterized by sticking. As the metal advances toward the die exit, the metal starts to slide along the bearing and, if the bearing is long enough, it resembles plug flow. Moreover, it was shown that a long bearing

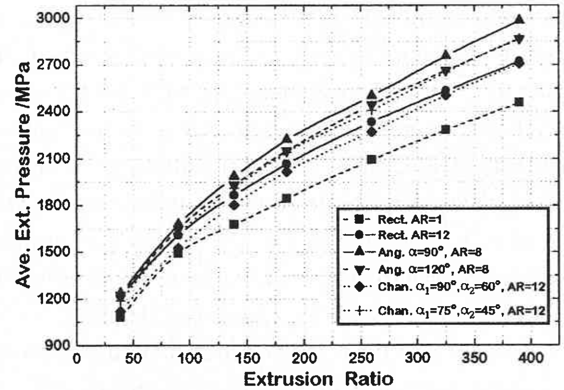

Fig. 10 Relationship between P_{Av} and ER for various cross sections.

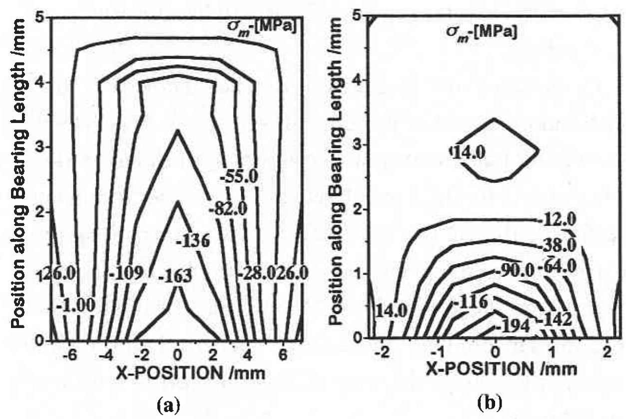

Fig. 11 σ_m distribution for a rectangular section, AR = 1, Z_B = 5 mm **(a)** ER = 39 **(b)** ER = 390.

assures the straightness of the material at the die exit, however the extrusion pressure increases.

It was observed that the most influential parameter is the position of the die opening with respect to the billet axis. The distribution of the axial velocity is very sensitive to the eccentricity of the die opening position.

Finally, it is concluded that optimal bearing length and optimal position can be successfully simulated by numerical analysis so that the lengths of the bearing lands can be kept short and the ram forces comparatively low. Furthermore, metal-flow related defects as well as the soundness of the product can be successfully predicted.

(Manuscript received, March 22. 1996)

References

1) M. Kiuchi et.al.: Proc. JSTP Autumn Conf. (1995), 285.
2) M. Kiuchi et.al.: Proc. JSTP Autumn Conf. (1995), 287.